

Supporting Information

Visible-light-driven sonophotocatalysis for enhanced Cr(VI) reduction based on mixed-linker zirconium-porphyrin MOFs

*Wenhao Liu,^a Zhifen Guo,^b Zhi Jin,^a Dashu Chen,^{*a} Teng Lu,^a Peiyun Jia^a and
Hongzhu Xing^{*b}*

*^aCollege of Chemistry, Chemical Engineering and Resource Utilization, Key
Laboratory of Forest Plant Ecology Northeast Forestry University, No. 26 Hexing
Road, Harbin, 150040, China*

E-mail: chends410@nenu.edu.cn

*^bProvincial Key Laboratory of Advanced Energy Materials, College of Chemistry,
Northeast Normal University, No. 5268 Renmin Street, Changchun, 130024, China*

E-mail: xinghz223@nenu.edu.cn

Materials

Zirconium (IV) chloride ($ZrCl_4$) (99%, TCI), acetic acid (99.5%, Innochem), potassium dichromate (99.5%, Acros), tetrakis(4-carboxyphenyl)-porphyrin (TCPP), benzoic acid (99.5%, Aladdin), 4,4',4''-(2,4,6-trimethylbenzene-1,3,5-triyl)tribenzoate (TBTB, Leyan), 1,3,5-benzene(tris)-benzoate (BTB), potassium phosphate (99.5%, Innochem), potassium phosphate monobasic (99.5%, Innochem), 1,5-Diphenylcarbazide (DPC, 97%, Alfa), N,N-diethyl-1,4-phenylenediamine (DPD, 98%, Acros), horseradish peroxidase (POD, Aladdin), methacrylic acid (99%, Aladdin), Zirconium(IV) propoxide (ca. 70%, solution in propanol, Acros). Other reagents and chemicals were analytical purity and used as received without any further purification.

Characterization

Powder X-ray diffraction (PXRD) data was recorded on a Rigaku D-MAX 2550 diffractometer using Cu $K\alpha$ radiation, $\lambda = 0.15417$ nm) with 2θ ranging from 3° to 40° and a scanning rate of 5° min^{-1} at room temperature. N_2 sorption measurements were measured at the liquid nitrogen temperature, using a Micromeritics ASAP 2020 system. UV-Vis absorption spectra of liquid sample were recorded on a SHIMADZU UV-2550 spectrophotometer. UV-Vis spectra of solid-state samples were recorded on a HITACHI U-4100 spectrophotometer. The morphologies of samples were characterized by a field emission scanning electron microscopy (XL30ESEM-FEG, USA). The photoluminescence (PL) spectra were measured on FLSP920 fluorescence spectrometers. The valence state of Cr bound to PCN-134 and PCN-138 after catalytic process was analyzed based on X-ray photoelectron spectroscopy (XPS) spectra (Thermo Fisher Scientific, UK). EPR spectra were obtained on a JES-FA 200 EPR spectrometer; scanning frequency: 9.45 GHz; central field: 330 mT; scanning width: 10 mT; scanning power: 0.998 mW; scanning temperature: 25°C . The in situ EPR experiments were carried out using a 500 W xenon arc lamp where a 420 nm optical filter was used to cut off ultraviolet light. Photocurrent measurements were conducted on electrochemical workstation CHI 660E (ChenHua Instrument, Shanghai). Gas-phase products were monitored by GC-MS (Shimadzu Pro 2010). Photocurrent measurements were performed in a standard three-electrode system with the MOF-coated indium tin oxide as the working electrode, Pt and Ag/AgCl electrodes as the counter electrode and reference electrode, respectively. Aqueous solution of Na_2SO_4 (0.2 M) was used as electrolyte.

Synthesis of Zr_6 methacrylate oxoclusters

2 mL of Zirconium(IV) propoxide (ca. 70%, solution in *n*-propanol, 4.95 mmol) was mixed under an N_2 atmosphere with 2.5 mL of methacrylic acid (29.6 mmol) and stored in a closed Schlenk tube at ambient temperature for 11 days. After washed with *n*-propanol, the resulted samples were dried at 60°C .

Sonophotocatalytic reduction of Cr(VI) by Zr_6 methacrylate oxoclusters

In a typical process, 10 mL, $20 \text{ mg}\cdot\text{L}^{-1}$ Cr(VI) ($83 \text{ mg}\cdot\text{L}^{-1}$ for $Cr_2O_7^{2-}$) aqueous solution containing 10 mg Zr_6 methacrylate oxoclusters was placed in a Schlenk tube and the solution pH values were adjusted by H_2SO_4 . After being stirred for 60 min to reach adsorption–desorption equilibrium, the solution were irradiated by a 300 W Xe lamp with a 420 nm cut-off filter or six 10 W LED lamp (260-280 nm) under the power of ultrasound at 120 W. The left solution was measured by the absorbance at 540 nm using the DPC method to determine the concentration of Cr(VI).

Chromogenic detection of H_2O_2

The stock solution of DPD was prepared by dissolving 0.1 g DPD in a 10 mL 0.05 M H_2SO_4

solution. The peroxidase (POD) solution was prepared by dissolving 10 mg POD in 10 mL deionized water and was kept in a refrigerator for use. A potassium phosphate buffer solution was made by mixing 49.85 mL deionized water, 43.85 mL 1 M monobasic potassium phosphate, and 6.3 mL 1 M potassium phosphate. H₂O₂ detection solution was obtained from the eluents by repeatedly washing PCN-134 and PCN-138 with 2 mL of reaction solution. The eluents (0.5 mL) was mixed with 4.5 mL potassium phosphate buffer solution, 0.05 mL DPD and 0.05 mL POD. After coloration for 30 min, the obtained solutions were analyzed by UV-Vis spectroscopy.

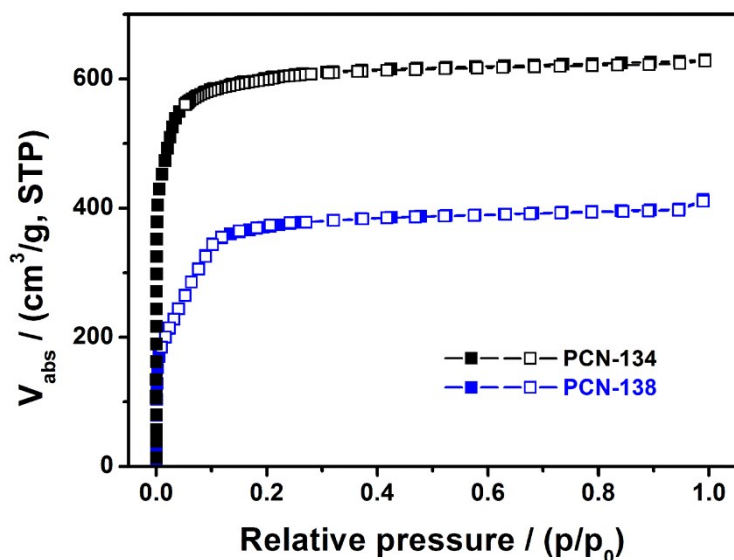


Figure S1. N₂ uptake of PCN-134 and PCN-138 measured at 77 K.

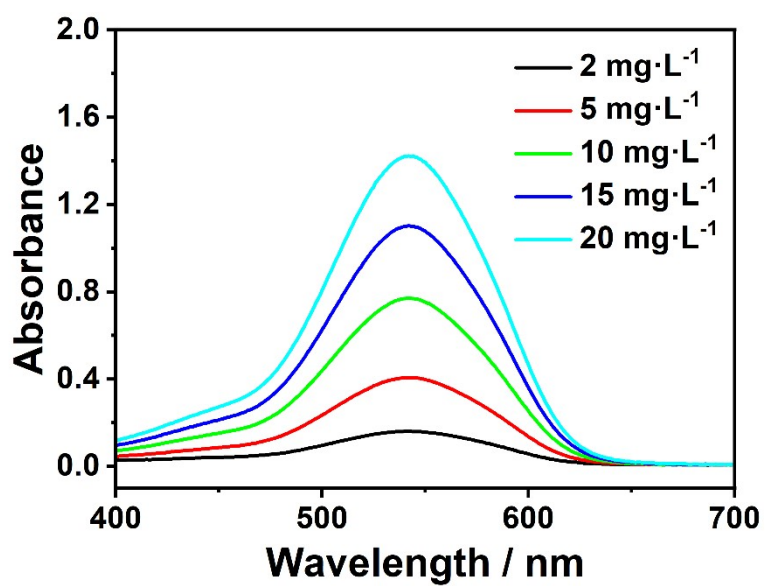


Figure S2. The UV-Vis absorption spectrum of Cr(VI)-diphenylcarbazide solution.

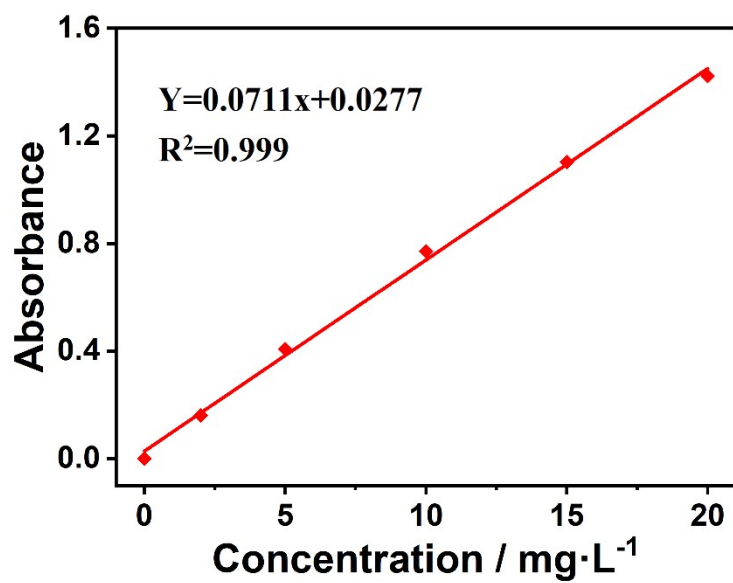


Figure S3. Calibration curve of Cr(VI)-diphenylcarbazide solution.

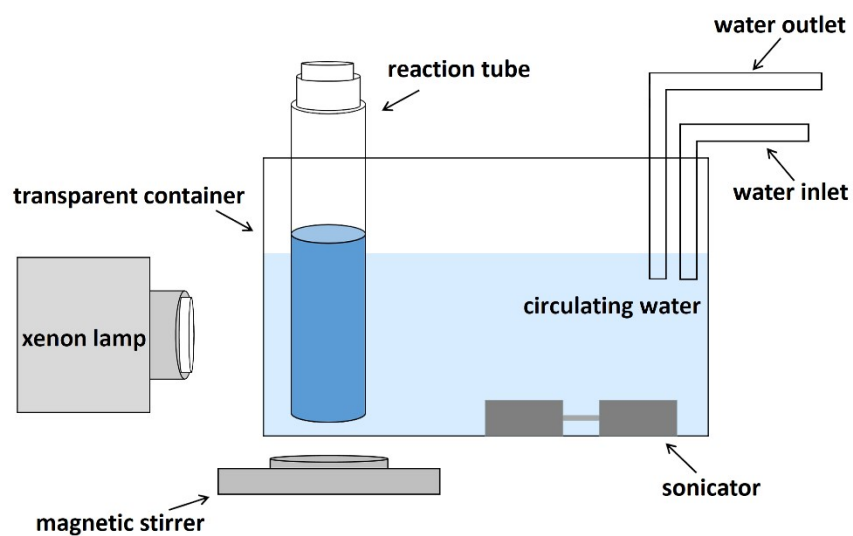


Figure S4. The equipment diagram of sonophotocatalytic experiments.

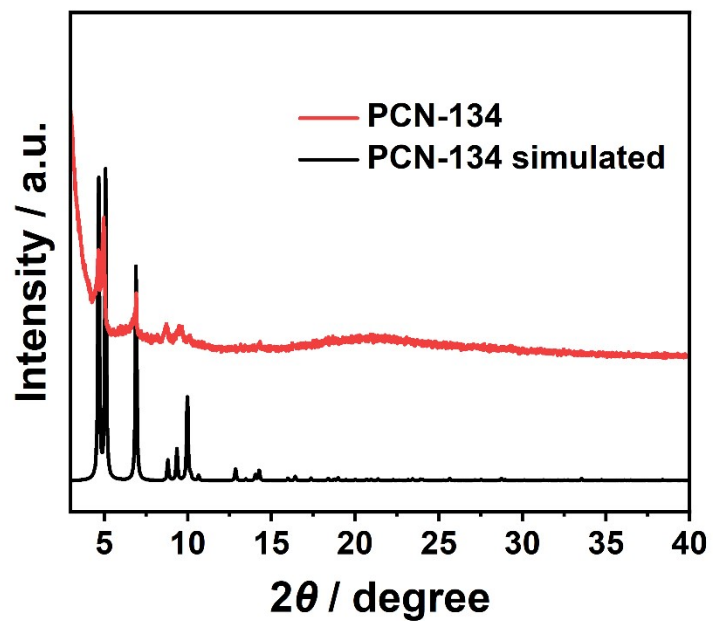


Figure S5. PXRD patterns of PCN-134 after 60 min sonophotocatalytic reaction and the simulated PCN-134.

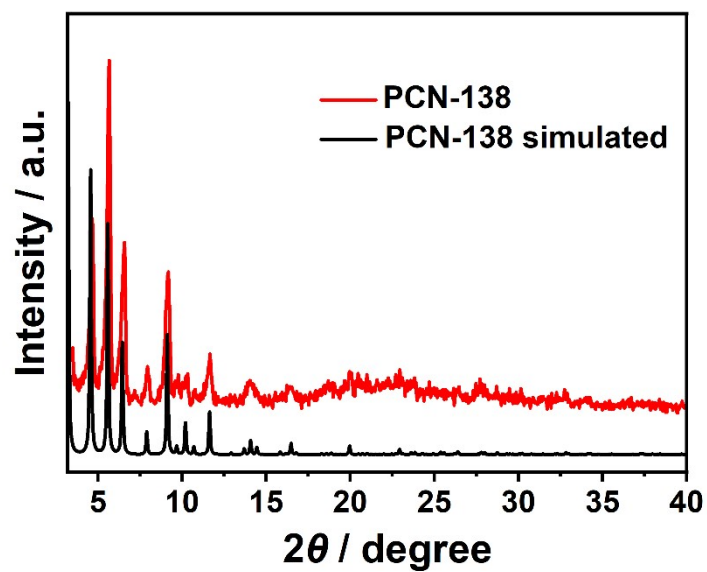


Figure S6. PXRD patterns of PCN-138 after 60 min sonophotocatalytic reaction and the simulated PCN-138.

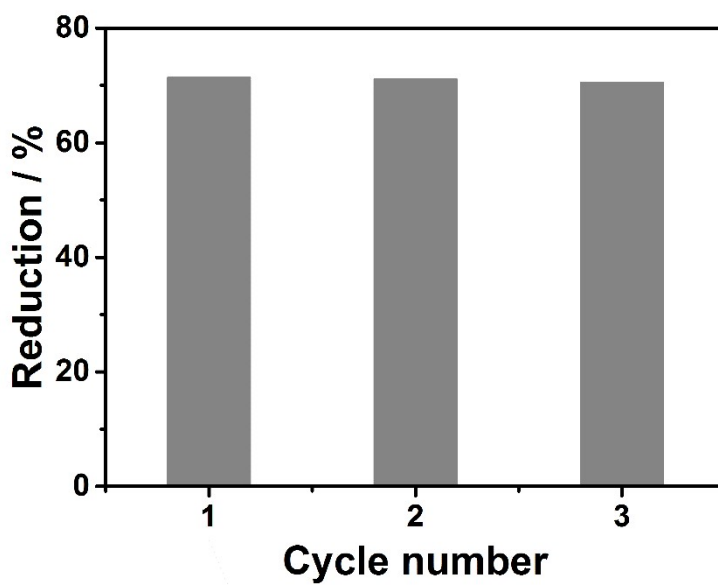


Figure S7. The cyclic tests of PCN-134 for sonophotocatalytic Cr(VI) reduction within 60 min.

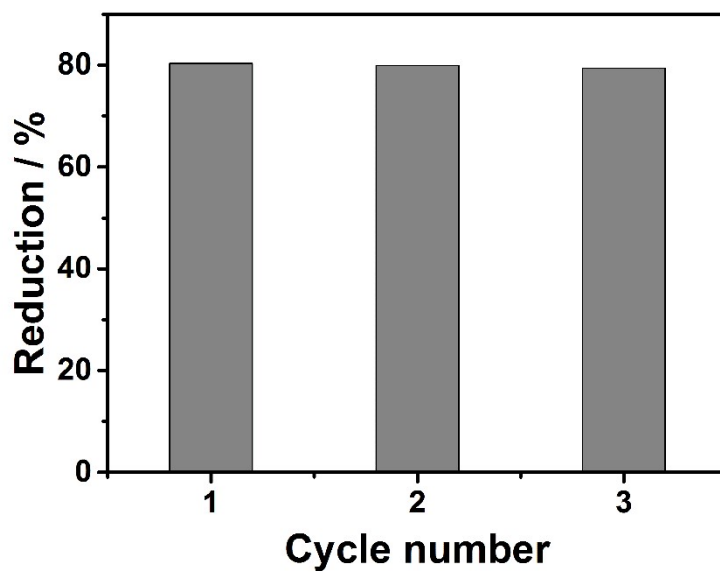


Figure S8. The cyclic tests of PCN-138 for sonophotocatalytic Cr(VI) reduction within 60 min.

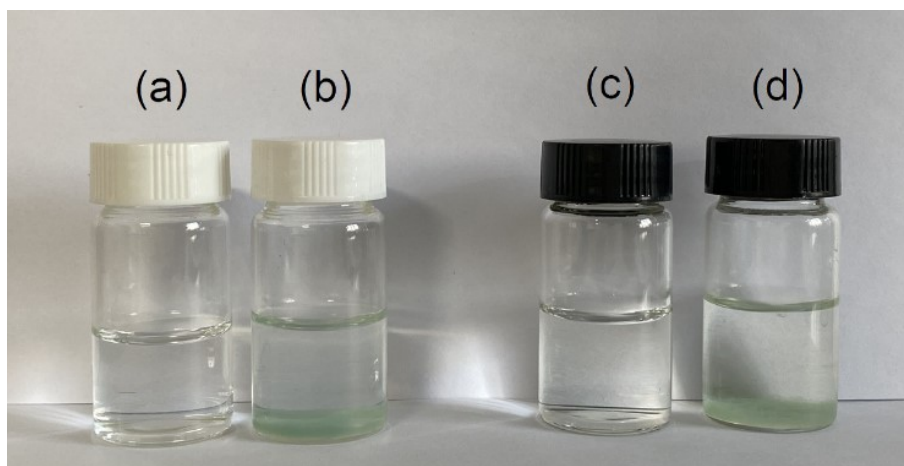


Figure S9. The photograph of reaction solution of 90 min sonophotocatalytic Cr(VI) reduction based on PCN-134 (a) non-treated (b) alkalized and PCN-138 (c) non-treated (d) alkalized.

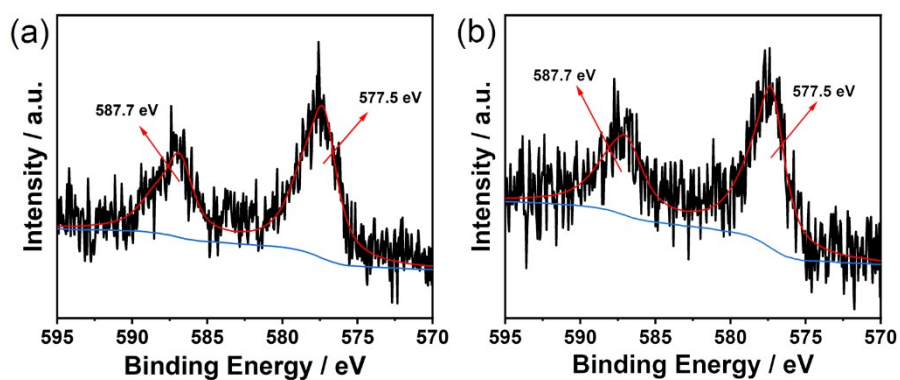


Figure S10. The spectra of XPS survey of PCN-134 and PCN-138 after sonophotocatalytic Cr(VI) reduction reaction. (a) PCN-134. (b) PCN-138.

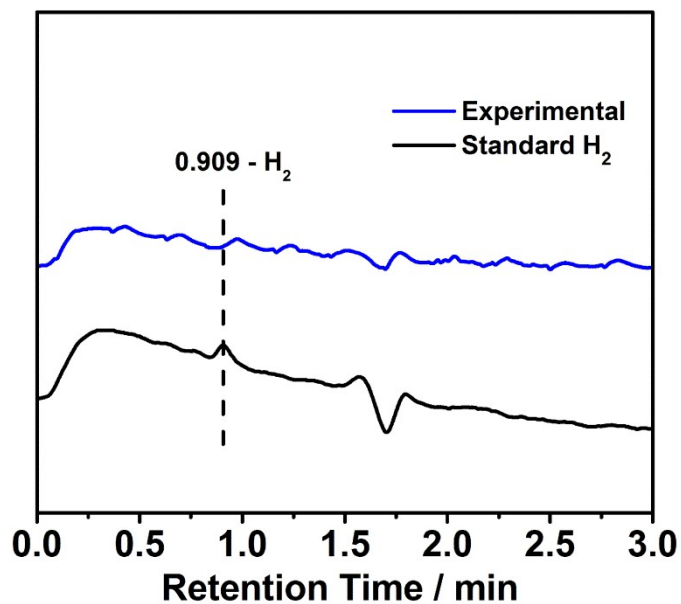


Figure S11. Gas chromatogram of catalytic system and standard hydrogen.

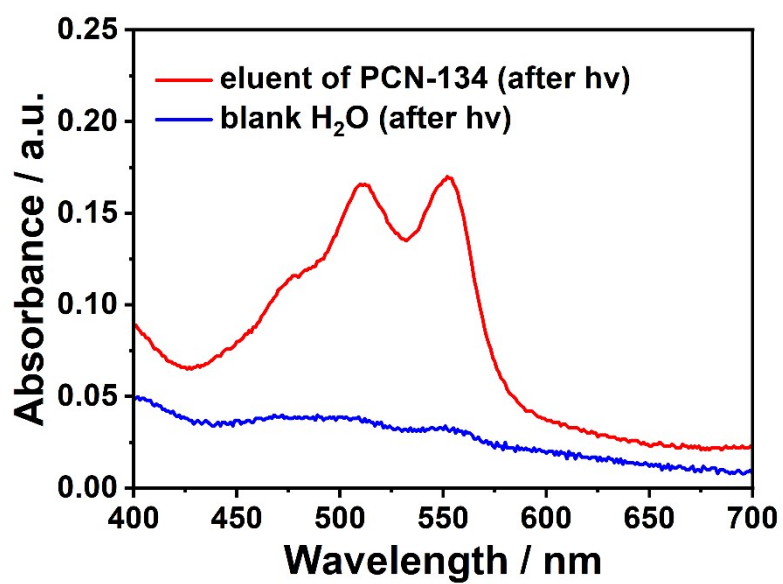


Figure S12. Chromogenic detection of H₂O₂ after sonophotocatalysis by the DPD/POD method.

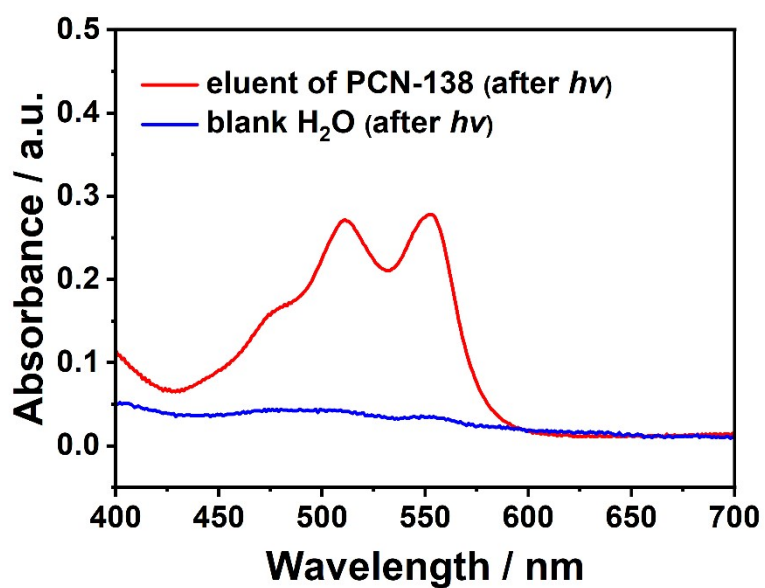


Figure S13. Chromogenic detection of H₂O₂ after sonophotocatalysis by the DPD/POD method.

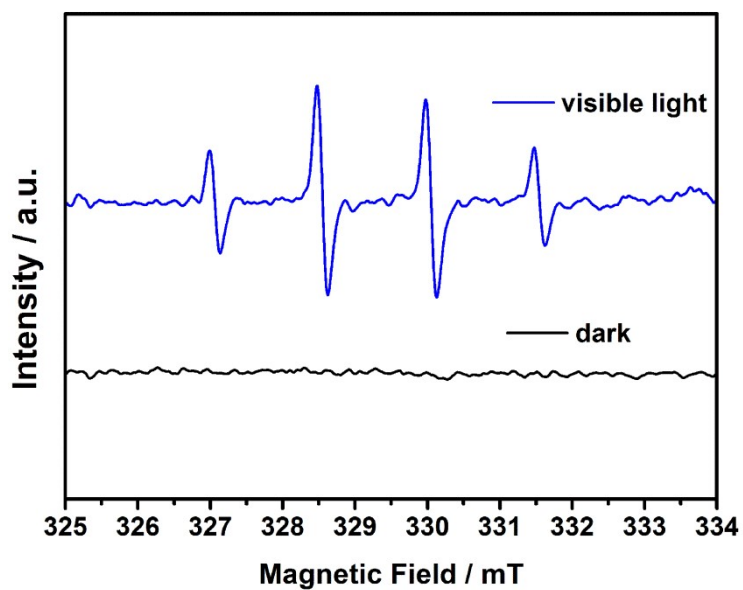


Figure S14. DMPO-assisting EPR spectra for the detection of possible radicals (black line: the liquid before photocatalytic reaction; blue line: the liquid after 5 min photocatalytic reaction).

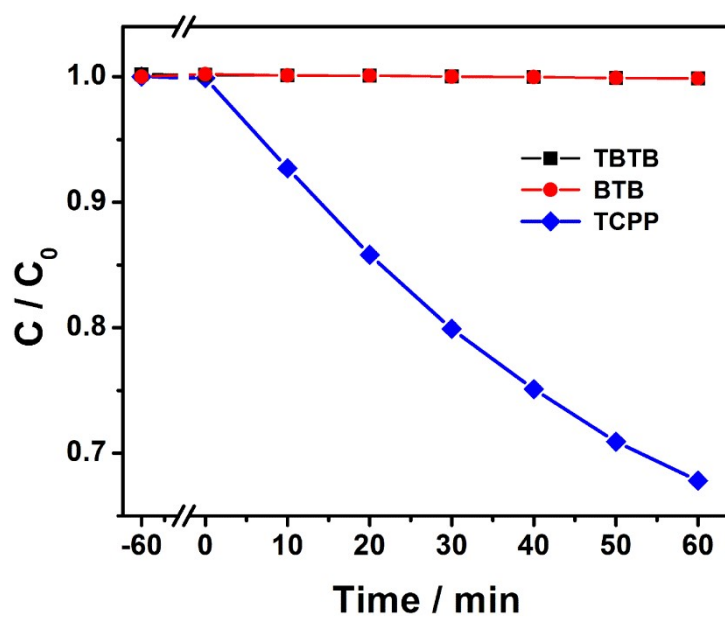


Figure S15. Sonophotocatalytic reduction of Cr(VI) over TBTB, BTB and TCPP ligands.

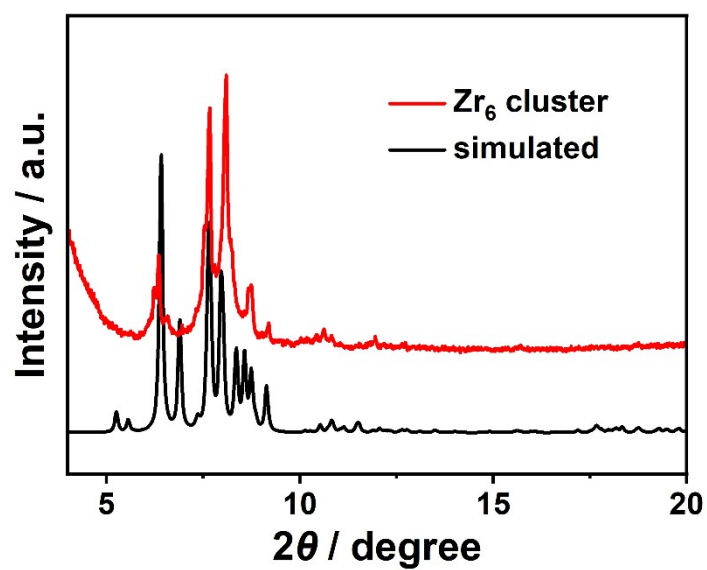


Figure S16. PXRD patterns of Zr_6 methacrylate oxoclusters and the simulated one.

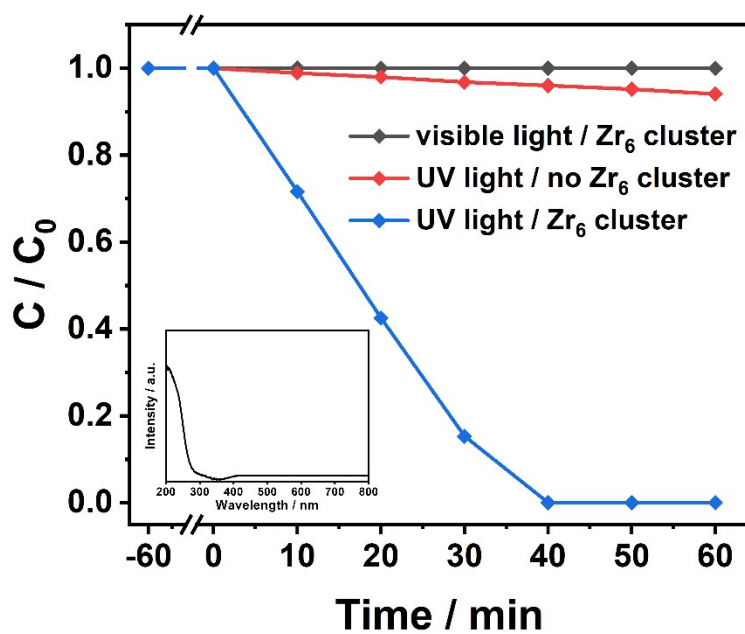


Figure S17. Zr_6 methacrylate oxoclusters mediated sonophotocatalytic reduction of Cr(VI) under different light irradiation (Insert: Solid UV-Vis absorption spectra of Zr_6 methacrylate oxoclusters).

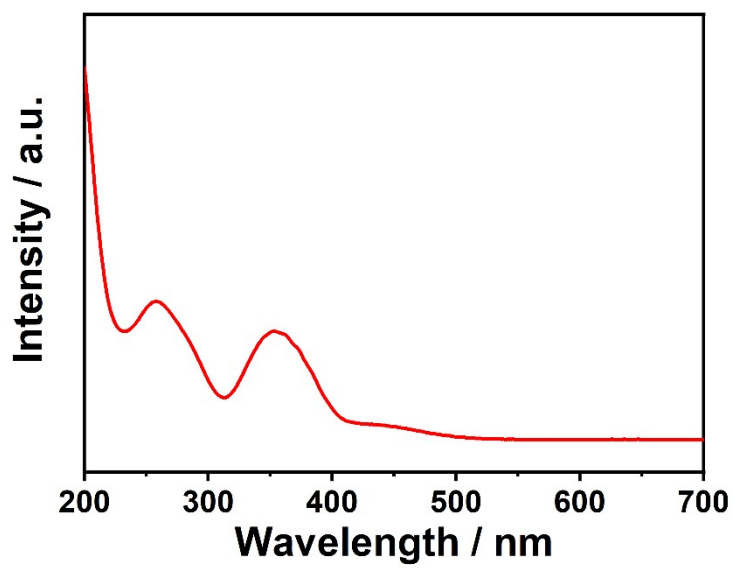


Figure S18. The UV-Vis absorption spectra of 20 mg·L⁻¹ Cr(VI) aqueous solution.